Organization and Structure of Clouds and Precipitation on the Mid-Atlantic Coast of the United States. Part VI: The Synoptic Evolution of a Deep Tropospheric Frontal Circulation and Attendant Cyclogenesis

JONATHAN E. MARTIN, JOHN D. LOCATELLI, AND PETER V. HOBBS

Atmospheric Sciences Department, University of Washington, Seattle, Washington

(Manuscript received 30 December 1991, in final form 12 September 1992)

ABSTRACT

Interactions between an upper-level frontal system and an initially weak surface cold front resulted in the production of a deep, precipitating frontal structure over the south Atlantic states on 26–27 January 1986. Attendant with the intensification of the frontal circulation was the development of an intense marine cyclone off the Delmarva peninsula. The increase in frontal-circulation strength is attributed to a favorable vertical superposition of the surface frontal trough and the upper-level frontogenetic horizontal deformation field that resulted in a deep column of divergence over the surface frontal trough. The surface cyclone developed partly, and indirectly, in response to the increase in warm-air advection in the lower stratosphere, which was directly related to an increase in the slope of the dynamic tropopause. The increase in the slope of the tropopause is hypothesized to have been the result of the combined effect of adiabatic advection of low tropopause height in the cold air of the upper trough and the latent heating associated with the onset of deep convection during the frontal development.

I. Introduction

The concept of fronts, which was introduced in the Norwegian cyclone model, provided insights into the relationship between the structure of extratropical cyclones and distribution of precipitation within these systems. Precipitation was ascribed to the upward motion of air over frontal surfaces (Bjerknes 1919; Bjerknes and Solberg 1921, 1922). Subsequently, the emphasis on frontal surfaces and the kinematics associated with them gave way to descriptions of frontal motions based on the dynamical processes that accompany frontogenesis. This shift in emphasis was formalized by Sawyer (1956) and Eliassen (1962), who viewed fronts as regions of continual frontogenesis rather than static boundaries between different air masses. In such regions, the vertical circulations commonly associated with fronts were shown to arise dynamically in response to accelerations along the fronts. These accelerations can result from an increase in the horizontal temperature gradient by differential horizontal advection.

In this paper we use a case study from the east coast of the United States to illustrate the evolution of a frontal circulation that eventually resulted in a deep band of precipitation. Involved in this evolution were a surface cold front and an upper-level front, originally located west of the surface front, which migrated rapidly through a developing long-wave trough. The upper front and upper-frontogenetic flow eventually caught up to, and became vertically superposed on, the surface front. The resulting enhanced vertical circulation rapidly transformed the whole system into a precipitation producer. In addition, the vigorous convection had a strong influence on the development of a surface cyclone through a combination of adiabatic and diabatic processes related to the slope of the "dynamic tropopause" [i.e., the tropopause defined in terms of potential vorticity—see Danielsen (1968)]. This work highlights the importance of upper-frontogenetic processes in generating precipitation and offers an alternative perspective from which to view the diabatic–dynamic interactions that characterize cyclogenesis in the extratropics.

In the next section we describe the synoptic situation and trace the history of the surface low pressure center, its associated surface cold front, and the upper-level front. Satellite and National Weather Service (NWS) radar datasets are used to trace the transformation in frontal precipitation that was produced by the superposition of the upper-level and surface fronts. In sections 3 and 4 we propose and discuss a mechanism for the development of the surface low pressure system.

Corresponding author address: Prof. Peter V. Hobbs, Department of Atmospheric Sciences, AK-40, University of Washington, Seattle, WA 98195.

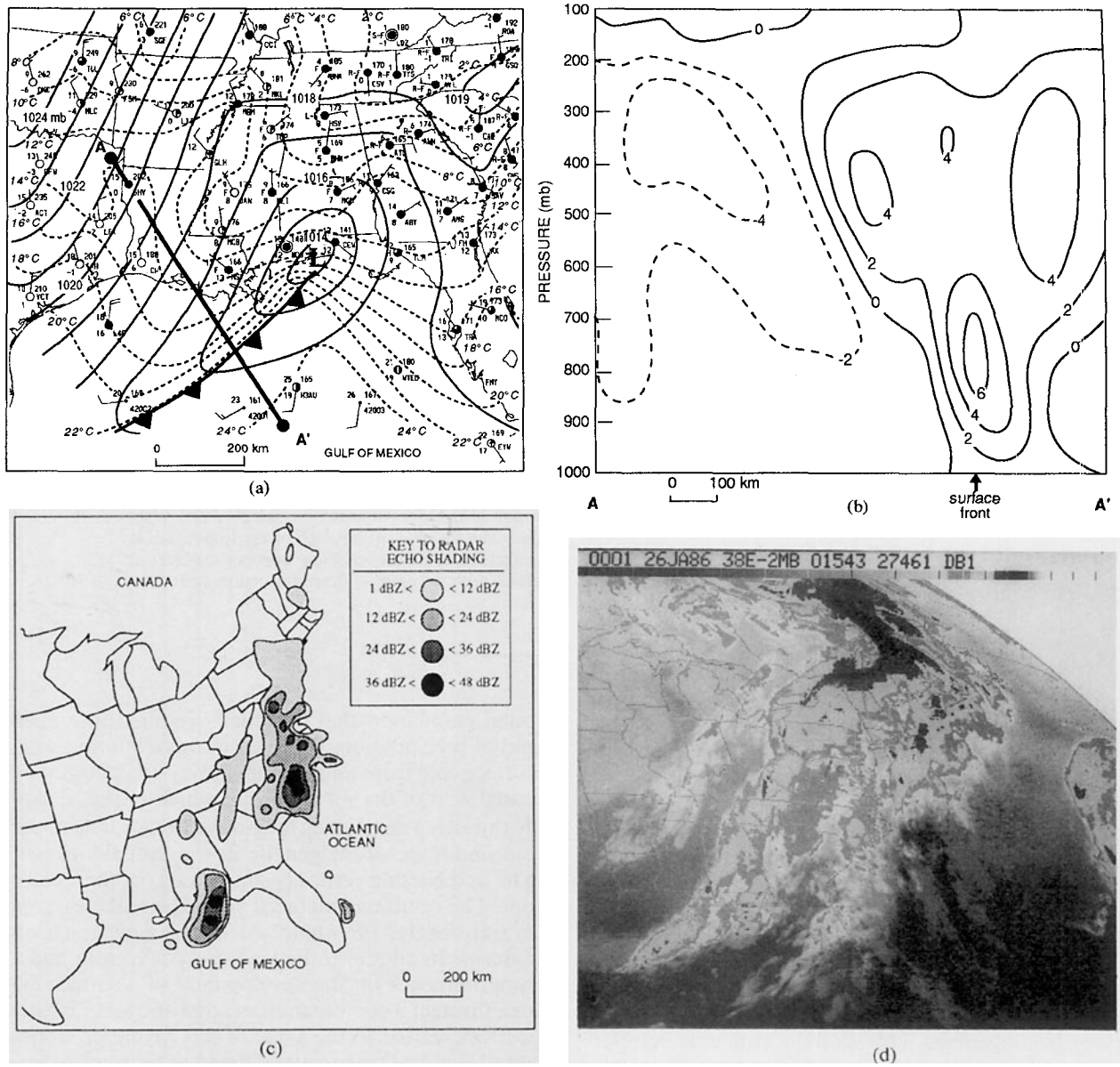

FIG. 1. (a) Sea level pressure and temperature analysis for 0000 UTC 26 January 1986. Solid lines are isobars (mb, contoured every 1 mb). Dashed lines are temperatures (°C, contoured every 2°C). Letter L marks the position of the surface low pressure center and conventional frontal symbol is used to indicate the position of the surface cold front. A cross section along line AA' is shown in (b). For each surface station the following data is shown: temperature (°C, upper left of the station symbol), dewpoint temperature (°C, lower left of station symbol), sky cover (in center of station symbol), wind direction and speed, and present weather. Sky cover is shown using the following symbols: open circle, clear; half-circle shaded, scattered cloud; unshaded vertical strip within otherwise shaded circle, broken cloud; fully shaded circle, overcast; and X, sky obscured. Wind speeds are indicated by: circle around a circle, calm; long barb, 5 m s^{-1}; short barb, 2.5 m s^{-1}; and flag, 25 m s^{-1}. Present weather symbols: R (rain), W (shower), L (drizzle), H (haze), S (snow), F (fog), ZR (freezing rain), BS (blowing snow), and K (smoke). A plus or minus sign after the precipitation type indicates heavy or light precipitation, respectively. (b) Vertical cross section along AA' in (a) of NGM 12-h forecast for vertical velocity (cm s^{-1}) valid at 0000 UTC 26 January 1986. Solid lines are upward vertical velocity and dashed lines are downward vertical velocity, (both contoured every 2 cm s^{-1}). (c) NWS radar data at 0000 UTC 26 January 1986. (d) Infrared satellite image at 0000 UTC 26 January 1986.

2. Synoptic analysis

a. 0000 UTC 26 January 1986

At 0000 UTC 26 January 1986 an incipient surface low pressure center was located at the extreme western edge of the Florida panhandle (Fig. 1a). The system was accompanied by a comparatively weak circulation. Trailing the low pressure center to its southwest was a shallow, precipitating cold front that extended across the Gulf of Mexico.

A vertical cross section along AA' in Fig. 1a is shown in Fig. 1b. This cross section lies perpendicular to the cold front over the Gulf of Mexico and was constructed using the Nested Grid Model (NGM) 12-h forecast dataset at 50-mb intervals in the vertical valid at 0000 UTC 26 January. It shows that the vertical circulation associated with the surface front was largely confined to the lower troposphere (below 700 mb) and a second circulation associated with the upper trough lay to its northwest at lower pressures. Despite its apparent shallowness, the NWS radar data at 0000 UTC (Fig. 1c), and the IR satellite image at the same time (Fig. 1d), revealed that significant convective activity was present along this front. The signatures evident along the East Coast in both the radar data and satellite image at this time were associated with an intense coastal front (Martin et al. 1990).

The 500-mb analysis (Fig. 2a) for 0000 UTC 26 January clearly shows a vigorous upper-level frontal zone near the vorticity maximum over Oklahoma and Texas. The development of this front has been described in detail by Martin et al. (1992). As described by Reed (1955), Reed and Sanders (1953), and many others since, a common by-product of the upper-level frontogenetic process is the downward protrusion of tropopause and lower-stratospheric air into the mid-troposphere (so-called *tropopause folding*). This occurred on 26 January 1986. The isentropic potential vorticity (IPV) can be used to define a "dynamic tropopause," since IPV is discontinuous across the tropopause (Danielsen 1968). Figure 2b shows a cross section from Monett, Missouri (UMN), to Oklahoma City, Oklahoma (OKC), to Stephenville, Texas (SEP), to Midland, Texas (MAF), along the line BB' in Fig. 2a. Potential temperature and temperature are taken from the sounding data; the IPV analysis is constructed using the NGM initialized data at 0000 UTC 26 January. These analyses demonstrate the thermodynamic and dynamic signatures characteristic of an upper-level front.

Figure 3 superposes the 500-mb and surface isotherm analyses taken from Figs. 1a and 2a. This diagram illustrates that the upper-level and surface fronts were nearly perpendicular to one another at 0000 UTC 26 January.

Differential thermal advection in a horizontal deformation field can lead to a thermally direct vertical circulation by increasing the magnitude of the horizontal temperature gradient and inducing accelerations along the front. Hence, in the absence of significant momentum advection effects it is relatively simple to infer the location of vertical circulations and frontal positions by locating regions where the horizontal flow on isobaric surfaces acts to concentrate the horizontal temperature gradient. The frontogenetic function

$$F_D = \frac{d}{dt}|\nabla\theta| = \frac{1}{|\nabla\theta|}\left[-\frac{\partial\theta}{\partial x}\left(\frac{\partial u}{\partial x}\frac{\partial\theta}{\partial x}+\frac{\partial v}{\partial x}\frac{\partial\theta}{\partial y}\right) - \frac{\partial\theta}{\partial y}\left(\frac{\partial u}{\partial y}\frac{\partial\theta}{\partial x}+\frac{\partial v}{\partial y}\frac{\partial\theta}{\partial y}\right)\right], \quad (1)$$

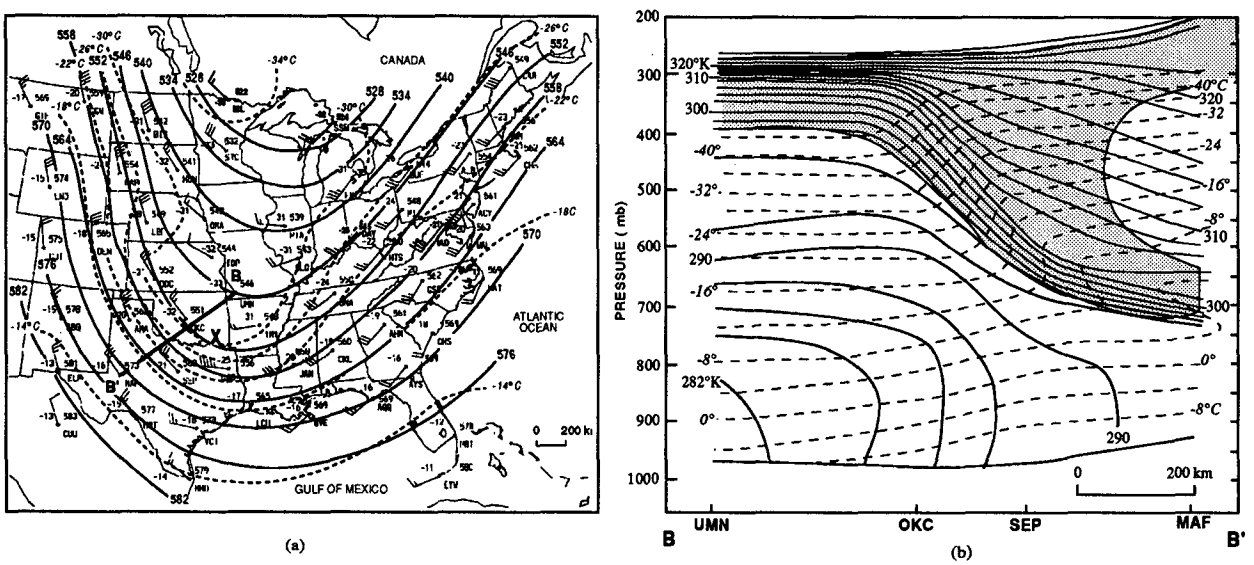

FIG. 2. (a) 500-mb analysis at 0000 UTC 26 January 1986. Solid lines are geopotential height (dam, contoured every 6 dam). Dashed lines are isotherms (°C, contoured every 4°C). Letter X marks the position of the 500-mb absolute vorticity maximum. A cross section along line BB' is shown in (b). For each station the following data are shown: station identifier (to the lower-right corner), geopotential height (dam, upper-right corner), and temperature (°C, upper-left corner). Wind speed indicated by: long barb, 10 m s^{-1} and flag, 25 m s^{-1}. (b) Vertical cross section from Monett, Missouri (UMN), to Oklahoma City, Oklahoma (OKC), to Stephenville, Texas (SEP), to Midland, Texas (MAF), along line BB' in (a). Solid lines are potential isotherms (K, contoured every 2 K). Dashed lines are isotherms (°C, contoured every 4°C). Shading indicates region with isentropic potential vorticity (IPV) > 1 PVU ($=10^{-6}$ m^2 s^{-1} K kg^{-1}).

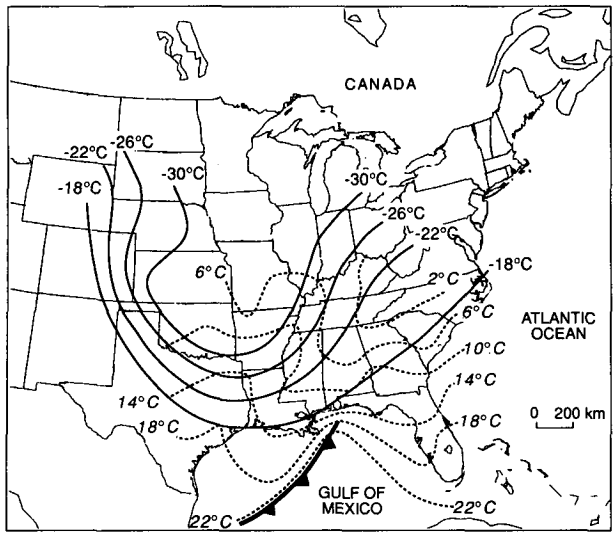

FIG. 3. Solid lines are 500-mb isotherms (°C, contoured every 4°C) from Fig. 2a. Dashed lines are surface isotherms (°C, contoured every 4°C) from Fig. 1a. Frontal symbol indicates position of the surface front.

represents the contribution to frontogenesis from the horizontal deformation, where the total derivative is

$$\frac{d}{dt} = \frac{\partial}{\partial t} + \mathbf{V}_2 \cdot \nabla_2. \qquad (2)$$

Here, F_D was calculated using the NGM total winds and temperatures on an 80-km grid mesh. Although this frontogenesis function does not include the important modifying effect of vertical velocities on the strength of the horizontal temperature gradient, it does, in general, make isolation of the regions and circumstances of vertical circulation forcing more obvious than the more complete 2D formulation (such as that introduced by Miller 1948).

Figure 4 shows F_D at 500 mb and the surface frontal position at 0000 UTC 26 January. It is evident that

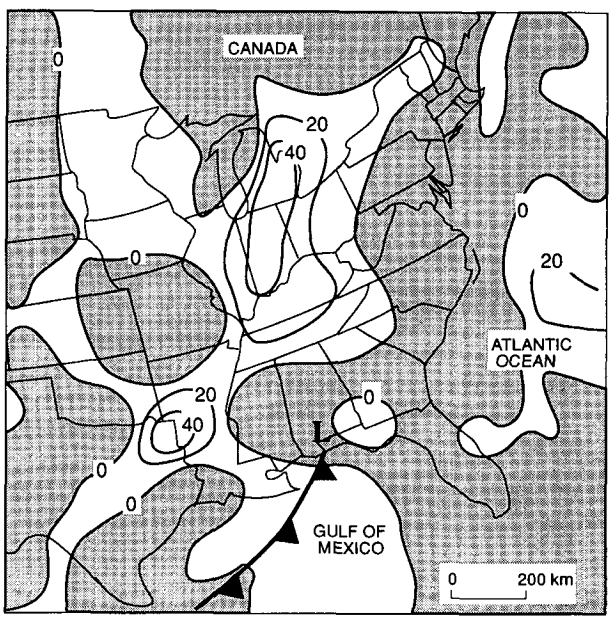

FIG. 4. The frontogenetic function F_D at 500 mb at 0000 26 January 1986. Shaded areas represent negative values of F_D. Solid lines are positive values of F_D (only positive values are labeled, in units of 10^{-11} K m^{-1} s^{-1}, and contoured every 20×10^{-11} K m^{-1} s^{-1}). Cold-frontal symbol shows the position of the surface cold front.

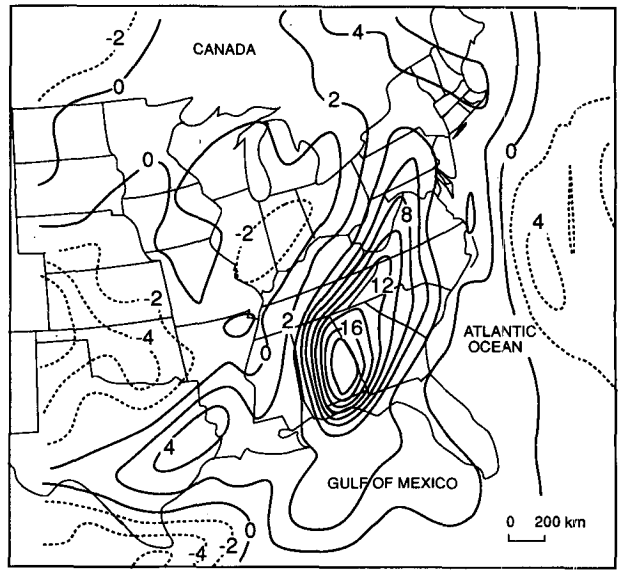

FIG. 5. NGM 12-h forecast of 500-mb vertical velocity valid at 0000 UTC 26 January 1986. Solid lines are upward vertical velocities; dashed lines are downward vertical velocities (cm s^{-1}, contoured every 2 cm s^{-1}).

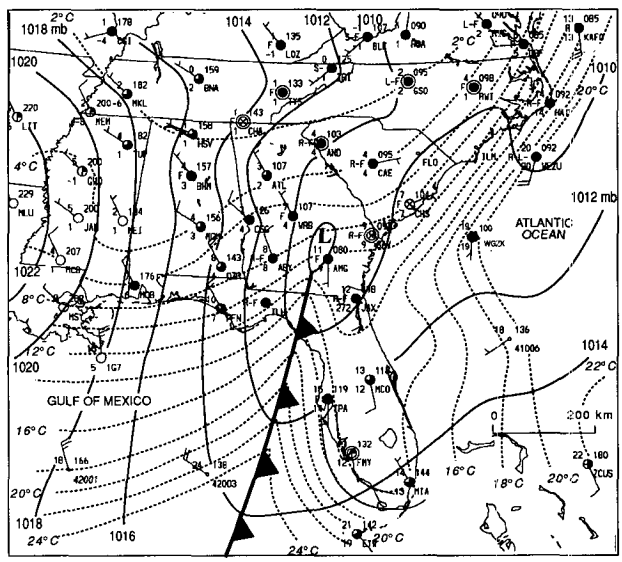

FIG. 6. As for Fig. 1a except for 1200 UTC 26 January 1986 and sea level pressure is contoured every 2 mb.

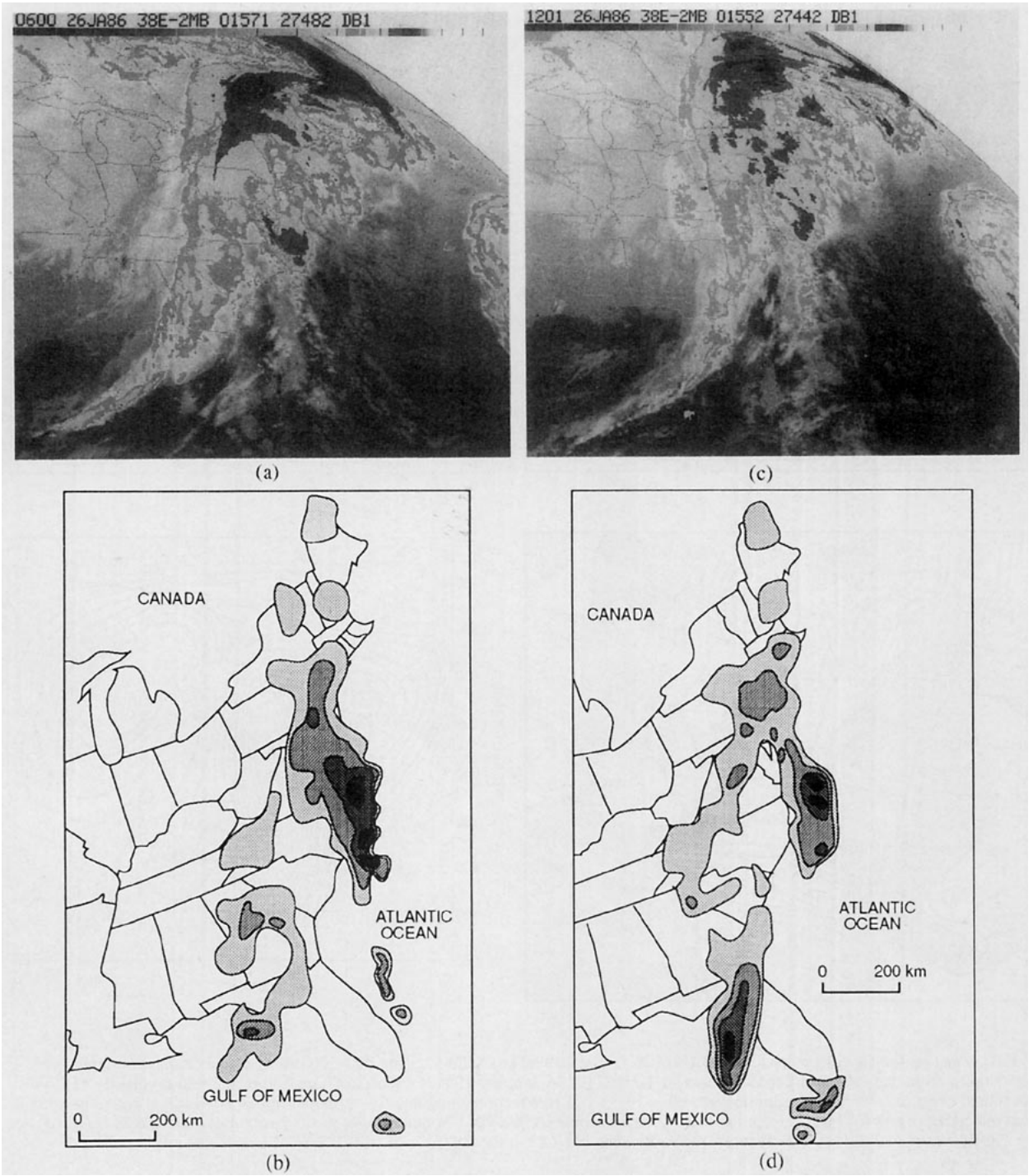

FIG. 7. (a) As for Fig. 1d except for 0600 UTC 26 January 1986. (b) As for Fig. 1c except for 0600 UTC 26 January 1986. (c) As for Fig. 1d except for 1200 UTC 26 January 1986. (d) As for Fig. 1c except for 1200 UTC 26 January 1986.

the inferred circulation forced by the upper-level frontogenesis did not exert any influence on the surface frontal circulation at this time. This inference is supported by the NGM vertical motion field shown in Fig. 5.

b. 1200 UTC 26 January 1986

Between 0000 and 1200 UTC 26 January 1986, the weak surface low pressure center and trailing surface cold front meandered east-northeast from the extreme

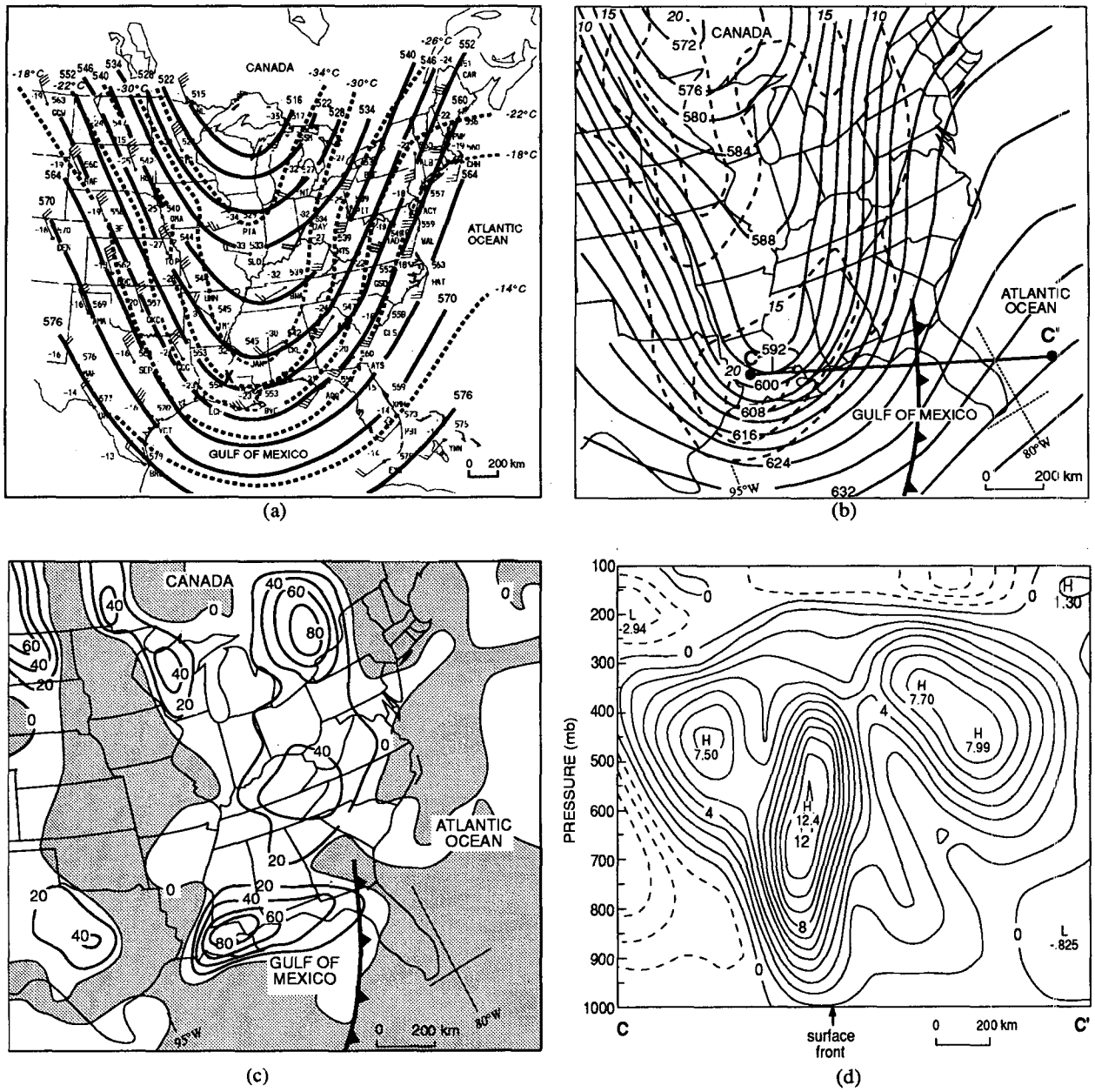

FIG. 8. (a) As for Fig. 2a except for 1200 UTC 26 January 1986. (b) Solid lines are 700–300-mb thickness (dam, contoured every 4 dam) taken from the NGM initialized dataset at 1200 UTC 26 January 1986. Dashed lines are 500-mb absolute vorticity (10^{-5} s^{-1}, contoured every 5×10^{-5} s^{-1}) beginning with 10×10^{-5} s^{-1}. Cross section along line *CC'* is shown in Fig. 8d. Surface frontal position is also indicated. (c) As for Fig. 4 except for 1200 UTC 26 January 1986. Cold-frontal symbol shows position of surface cold front. (d) As for Fig. 1b except at 1200 UTC 26 January 1986 and along line *CC'* in Fig. 8b.

western edge of the Florida panhandle to southern Georgia, near Waycross (Fig. 6). During this 12-h period, the central pressure dropped only 5 mb, from 1013 to 1008 mb, and the initially vigorous convective precipitation associated with the surface front weakened considerably, as is evident in the radar summaries (Fig. 7).

At 500 mb, the upper-level front and absolute vorticity maximum had encroached slightly further upon the surface system (Fig. 8a). Sutcliffe (1947) showed that a controlling factor for surface development in the quasigeostrophic framework is absolute vorticity advection by the thermal wind. The 700–300-mb thickness and 500-mb absolute vorticity, from the NGM

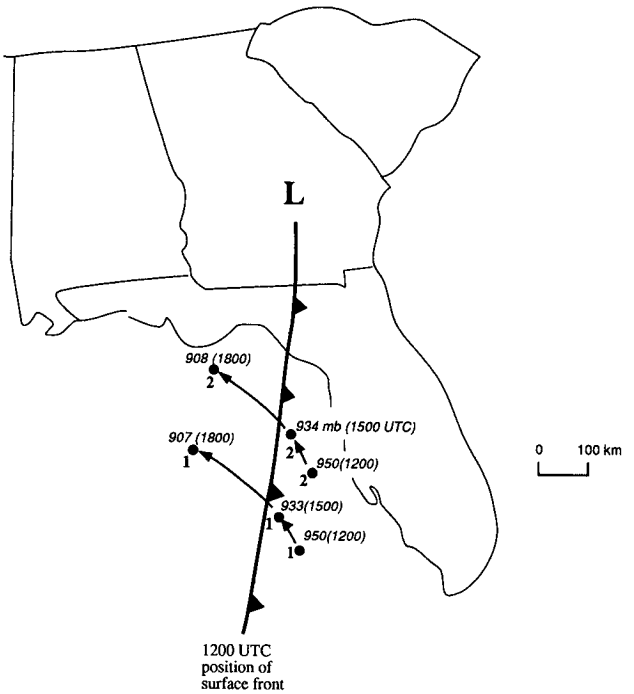

FIG. 9. Six-hour trajectories relative to the cold front calculated using NGM forecast data from 1200 UTC to 1800 UTC 26 January 1986. Trajectories were begun at 950 mb and the isobaric level is indicated at the beginning, middle, and ending points of each trajectory. The geographical background represents the synoptic setting at the *initial* time (1200 UTC) of the trajectories.

initialization at 1200 UTC, indicate that at this time the upper-level front, a feature characterized by its strong horizontal shear and thermal wind, and therefore a preferred region for quasigeostrophic forcing of vertical motion, was not close enough to the surface low to contribute to its development nor to that of the surface front (Fig. 8b). The deformation contribution to frontogenetic lifting at 500 mb was still quite separate from the dynamics of the surface front (Fig. 8c), although the circulation associated with the surface front had increased in strength by that time (Fig. 8d).

Trajectory analyses (constructed from successive 6- and 12-h forecast datasets from the NGM) showed only slight lifting along the leading edge of the surface front from 1200 to 1800 UTC 26 January. Figure 9 shows trajectories relative to the front for two air parcels in the boundary layer that originated just east of the surface front at 1200 UTC and 950 mb.

c. *1800 UTC 26 January*

A rapid transformation occurred in the frontal cloud band between 1200 and 1800 UTC 26 January, with an attendant increase in the precipitation intensity, as shown in Fig. 10. Notice, in particular, the appearance of a new level 4 echo on the South Carolina coast at 1500 UTC (Fig. 10b). This intense convection, which did not exist in that region at 1200 UTC (see Fig. 7d), was the first response to the vertical superposition of the upper and lower baroclinic features. The sea level pressure field was still largely ill-defined over the Carolinas at 1800 UTC, with dual low pressure centers near Atlantic City, New Jersey (ACY), and Wilmington, North Carolina (ILM). The low pressure center near Wilmington is the feature of interest, since its trailing front is the front that we have been tracking (Fig. 11a).

The 500-mb analysis at 1800 UTC shows that the upper-level front, and the associated vorticity maximum, had become almost parallel to the alignment of the surface front (Fig. 11b), suggesting that the upper forcing was now acting in concert with the convergence at the surface trough. The 700–300-mb thickness and 500-mb vorticity fields suggest that quasigeostrophic forcing associated with the upper-level front had become parallel to and to the west of the surface front, thereby contributing to its development (Fig. 11c). Interestingly, the maximum quasigeostrophic forcing associated with the upper feature was well to the southwest of the surface low. This may explain the lack of organization exhibited by the sea level pressure field up to 1800 UTC.

Upper-level frontogenesis also contributed to lifting in the middle troposphere above the location of the surface front at 1800 UTC. Figure 12 shows that the 500-mb deformation frontogenesis at 1800 UTC was finally in a position to enhance the frontal lifting already associated with the surface front. A vertical cross section of the deformation frontogenesis along the line *DD'* in Fig. 12a is shown in Fig. 12b. The westward sloping column of frontogenesis seen in this analysis resulted in a deep column of divergence (not shown) directly over, and sloping westward from, the surface frontal position. The result was a vertical circulation extending through the depth of the troposphere, as shown in Fig. 12c. This vertical motion produced the deep, vigorous precipitating clouds shown in Fig. 10.

Six-hour, front-relative trajectories, originating just east of the surface frontal position at 1800 UTC, demonstrate the important effect on the vertical motion produced by the favorable vertical superposition of the surface front and the upper-level frontogenetic forcing (Fig. 13). Air parcels originating ahead of the surface front experienced a displacement on the order of 120 mb from 1800 UTC 26 January to 0000 UTC 27 January (compared to less than 50 mb from 1200 to 1800 UTC 26 January when the upper frontogenesis was not in a position to influence the surface front).

d. *0000 UTC 27 January 1986*

The continued development of the convection associated with this frontal structure after 1800 UTC is

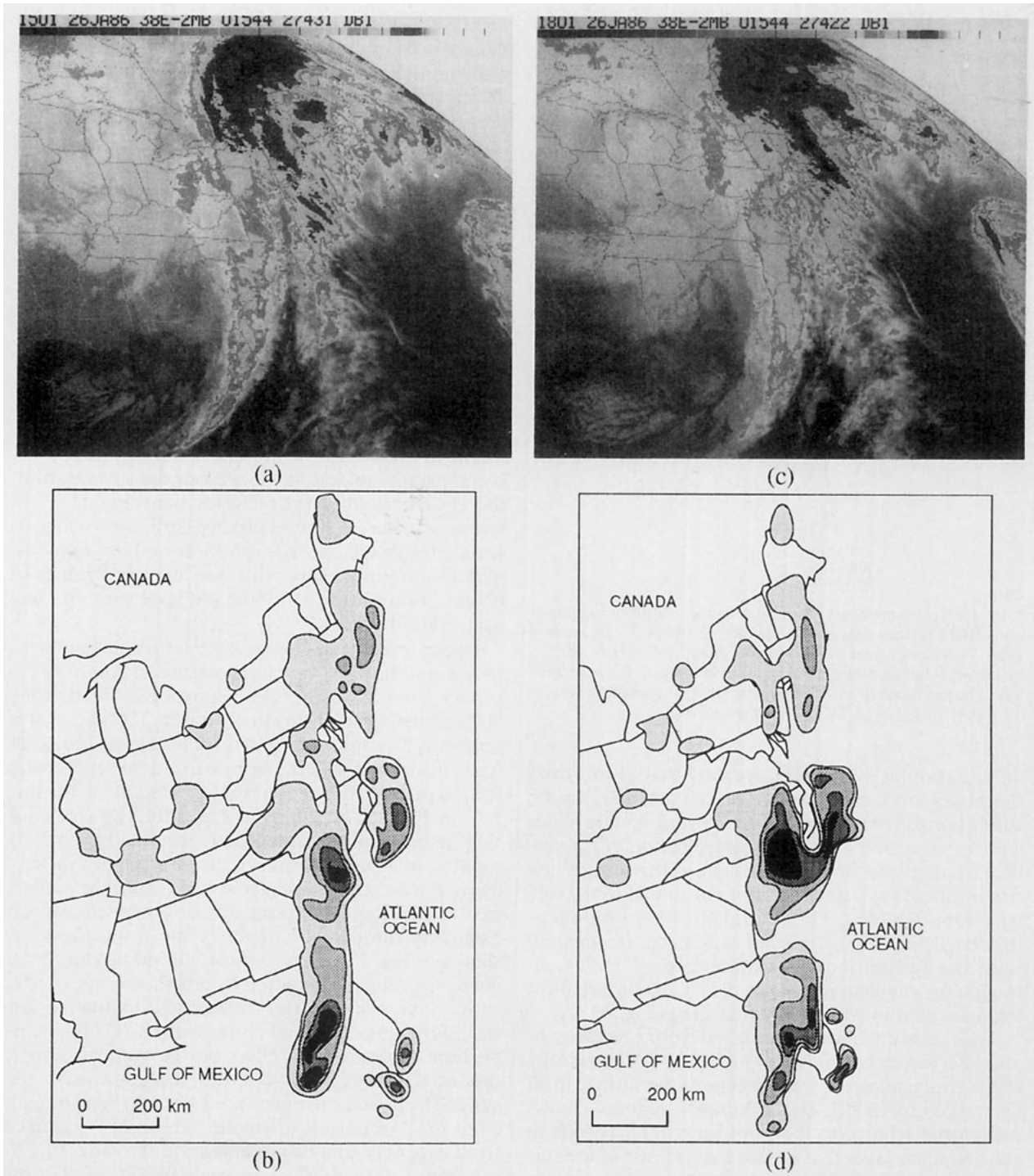

FIG. 10. (a) As for Fig. 1d except for 1500 UTC 26 January 1986. (b) As for Fig. 1c except for 1500 UTC 26 January 1986. (c) As for Fig. 1d except for 1800 UTC 26 January 1986. (d) As for Fig. 1c except for 1800 UTC 26 January 1986.

shown in Fig. 14. By 0000 UTC 27 January the previously complex and disorganized sea level pressure field had begun to take shape. An elongated trough of low pressure extended south from Atlantic City, New Jersey (ACY), to just offshore of Morehead City, North Carolina (MRH), and two low pressure centers, each with central pressure of 999 mb, occupied the extremities of the trough. Large pressure falls were occurring just offshore of Cape Hatteras, North Carolina (HAT), and the Delmarva peninsula. The surface front had

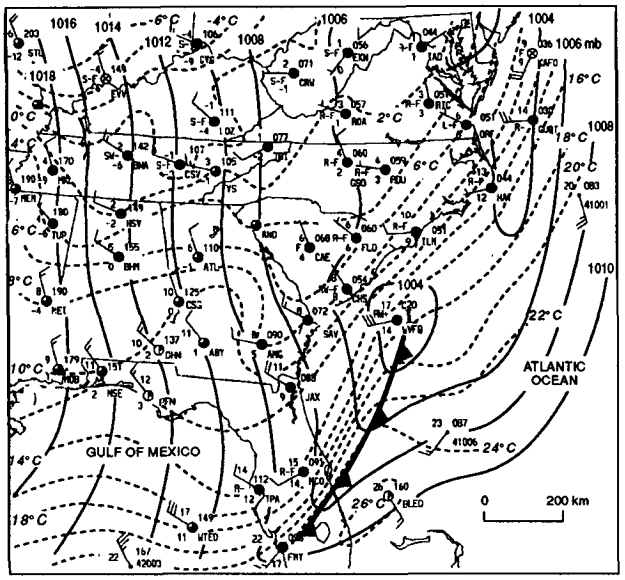

(a)

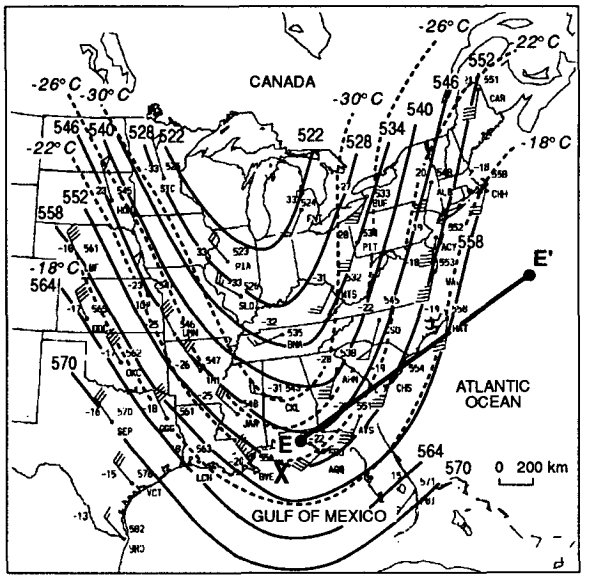

(b)

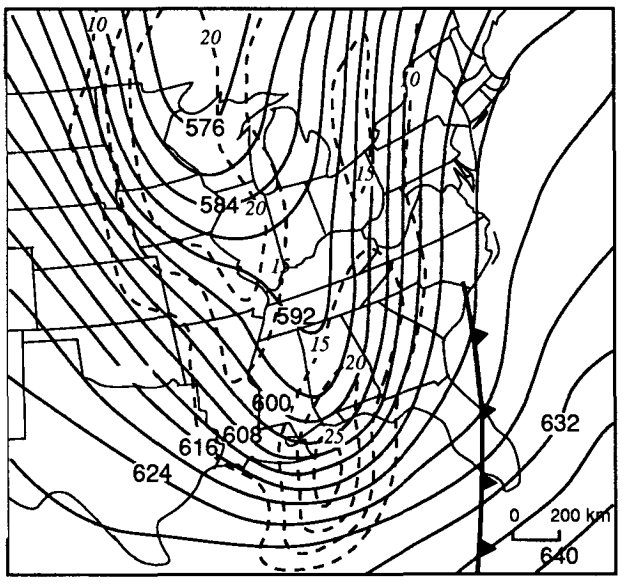

(c)

FIG. 11. (a) As for Fig. 1a except for 1800 UTC 26 January 1986. (b) As for Fig. 2a except for 1800 UTC 26 January 1986. Line *EE'* indicates the plane of the cross sections shown in Figs. 18a and 18b. (c) As for Fig. 8b except for 1800 UTC 26 January 1986.

crossed the entire length of the Florida peninsula by 0000 UTC and was vigorous. This is evidenced by the rapid drop in temperature and rise in pressure experienced by stations along the east coast of Florida, such as Miami (MIA), where the temperature fell from 23°C (73°F) at 1800 UTC to 14°C (58°F) at 0000 UTC while the pressure rose 3 mb in the same time with a dramatic veering of the wind (Fig. 15a). Further evidence for the strength of the surface front is provided by the field of surface F_D (Fig. 15b), which was quite vigorous at this time.

At 500 mb, the upper frontal zone, although weakened by the vertical circulation associated with it (shown in Fig. 15d), was still evident in the temperature and wind fields at 0000 UTC (Fig. 15c). The 700–300-mb thermal wind advection of 500-mb absolute vorticity (Fig. 15e) was now acting even more vigorously to assist the development of the surface front, although it was not in the most favorable position for development of the surface low off Cape Hatteras. The vigorous convection may have contributed more importantly to the subsequent development, in a manner to be described later. The trajectories and frontogenesis patterns at 0000 UTC 27 January were similar to those at 1800 UTC.

e. 0600 UTC 27 January

The sea level pressure field at 0600 UTC 27 January shows that the surface cyclone deepened by 10 mb be-

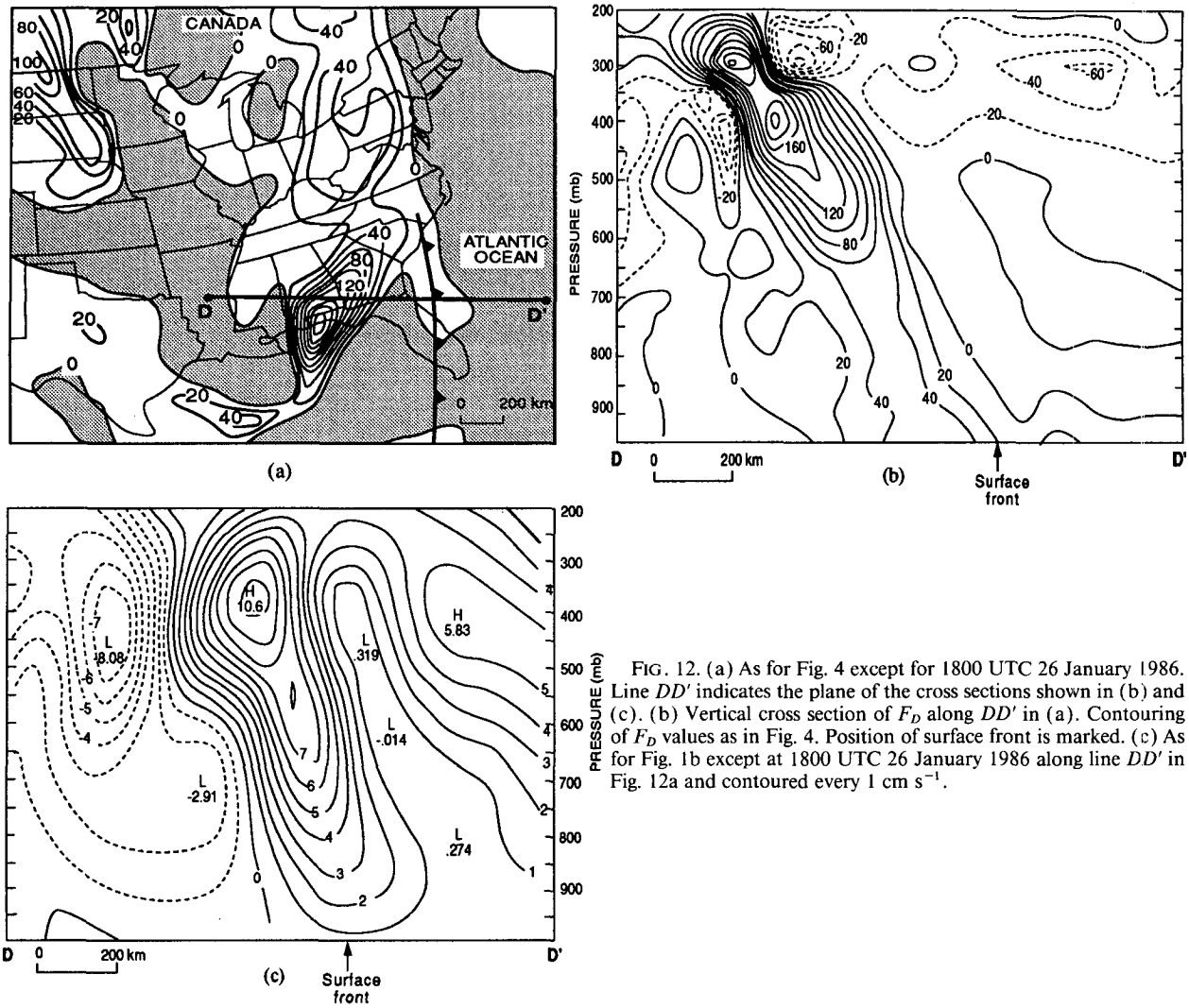

FIG. 12. (a) As for Fig. 4 except for 1800 UTC 26 January 1986. Line DD' indicates the plane of the cross sections shown in (b) and (c). (b) Vertical cross section of F_D along DD' in (a). Contouring of F_D values as in Fig. 4. Position of surface front is marked. (c) As for Fig. 1b except at 1800 UTC 26 January 1986 along line DD' in Fig. 12a and contoured every 1 cm s^{-1}.

tween 0000 and 0600 UTC (Fig. 16a). A low pressure center of considerable strength (989 mb) was located 100 n mi offshore of Salisbury, Maryland, and the surface front had moved rapidly eastward to a position south of the new low pressure center. Buoy 41001 had a temperature drop of 5°C (9°F) with the frontal passage, in spite of the extremely high temperature (21°C) of the Gulf Stream at that location; this attests to the strength of the front at this time. The entire mid-Atlantic states and southern New England states experienced intense pressure falls over the 3 h leading up to 0600 UTC. Boston, Massachusetts (BOS), some 300 n mi ahead of the surface low, experienced a 6.8 mb drop in pressure from 0300 to 0600 UTC.

The 700–300-mb thermal wind advection of 500-mb absolute vorticity (Fig. 16b) contributed strongly to the development of the surface front, although it still cannot be implicated in the rapid development of the surface cyclone since the maximum forcing was not collocated with the region of maximum pressure falls ahead of the cyclone. Vigorous convection was occurring far enough off the coast of North Carolina that a true radar depiction of its intensity was not possible; it can be inferred only roughly from the satellite imagery (Fig. 16c). The frontogenesis patterns and trajectories at 0600 UTC 27 January were similar in structure to, but of larger intensity than, those at 1800 UTC 26 January.

3. Mechanism for the development of the surface low

Between 1800 UTC 26 January and 0600 UTC 27 January the surface low pressure system, with which we are concerned here, deepened from 1002 to 989 mb. In fact, a 10-mb deepening occurred between 0000

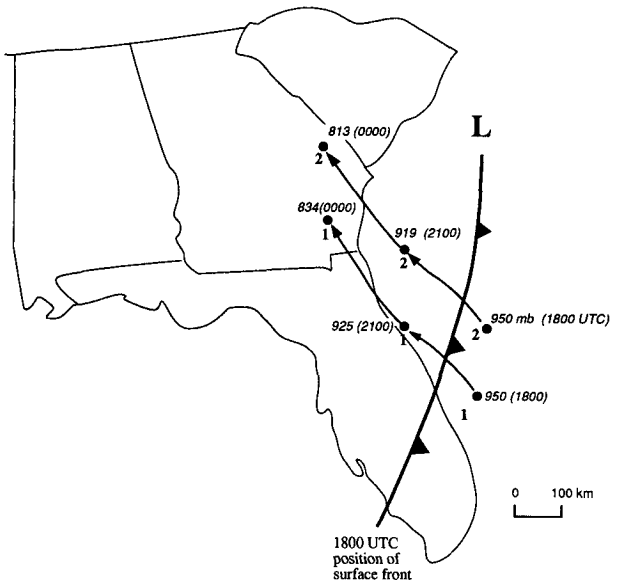

FIG. 13. Six-hour trajectories relative to the surface cold front beginning at 1800 UTC 26 January 1986 and ending at 0000 UTC 27 January 1986. Calculated as for Fig. 9 with the appropriate set of forecast data from the NGM. The geographical background represents the synoptic setting at the initial time (1800 UTC) of the trajectories.

and 0600 UTC. Two important observations with a bearing on this development are: 1) the development was initiated simultaneously with the explosion of deep convection along the surface front (see Fig. 14); and 2) the development occurred rather remotely from the maximum midtropospheric thermal wind advection of absolute vorticity (see Figs. 15e and 16b), which is the controlling factor for development in quasigeostrophic theory (Sutcliffe 1947).

Boyle and Bosart (1986) examined the effect of tropopause steepness on the rapid development of an East Coast winter storm. Recently, Hirschberg and Fritsch (1991) have reviewed and formalized the theory of tropopause steepening and its effects on surface cyclonic development via the hypsometric relationship, thereby resurrecting the ideas of Dines (1911) and others. An air column with a low tropopause height [equivalently a column with a positive isentropic potential vorticity (IPV) anomaly aloft] is characterized by a relatively warm lower stratosphere. Since, in a baroclinic atmosphere, the strength of the wind increases with height up to the tropopause, strong positive temperature advection is likely to occur in the lower stratosphere just downstream of a low tropopause height. The hypsometric equation shows that local temperature tendencies affect thickness changes more if they occur at low pressures (i.e., near the tropopause) than if they occur at high pressures (near the surface). For instance, a 100-mb layer of air centered at the jet stream level will experience a larger increase in its thickness for a given amount of temperature increase than an equally massive layer centered at 950 mb. This is because less mass exists above the jet stream than above 950 mb (which is represented mathematically by the $\ln p$ dependence of the hypsometric integration). Increasing the thickness of an isolated atmospheric column tends to depress the higher pressure surface and raise the lower pressure surface. Thus, unbalanced pressure gradient forces are created at both the top and bottom of the layer; the magnitudes of these forces depend on the extent of the increase in thickness. This leads to the creation of a divergence–convergence couplet in the vertical. The compensating ageostrophic motions that result act to remove mass from the column; this is of fundamental dynamical importance for cyclonic development. The net effects of this removal of mass are to increase the upward vertical velocity in the column and to produce cyclonic vorticity through column stretching, both of which contribute to development. A steepening of the tropopause will normally result in an increase in the horizontal temperature gradient in the lower stratosphere, leading to larger warm advection in the lower stratosphere downstream of the steepening region. As a result of the accompanying thickness increase, tropopause steepening is often accompanied by increases in upper-level divergence and the attendant development of a cyclone at the surface.

One way of viewing tropopause steepening is through IPV analysis. Since the tropopause may be viewed as an IPV surface (Danielsen 1968), it is susceptible to fluctuations in height and slope due to adiabatic frontogenesis on an IPV surface (Hoskins and Berrisford 1988) and to Lagrangian changes in IPV. The latter are governed by the equation

$$\frac{d}{dt}(\text{IPV}) = -\boldsymbol{\eta}\cdot\nabla_3\theta_t + \text{friction} + \text{turbulence}, \quad (3)$$

where $\boldsymbol{\eta}$ is the 3D vorticity vector and $\nabla_3\theta_t$ the 3D gradient of diabatic heating. Thus, adding a diabatic heat source to the atmosphere in the middle or upper troposphere can dramatically affect the slope of the tropopause. Considering the vertical component of (3), we see that beneath (above) the level of maximum heating, IPV is produced (destroyed).

In strongly convective precipitation, the latent heats released by condensation and fusion can be considerable and they are usually concentrated at middle to upper levels. The vigorous convection associated with the frontal system between 2100 and 0600 UTC (Fig. 14) was a source of IPV at the surface and a sink of IPV above the level of maximum heating (probably the 700–400-mb layer). The diabatic destruction of upper-tropospheric–lower-stratospheric IPV was likely accelerated by the cooling at cloud top, which increased with the convective activity. In addition to these important diabatic effects, high-IPV air was being advected eastward in the cold air of the upper trough. In the vicinity of the convection, the rate of advection of

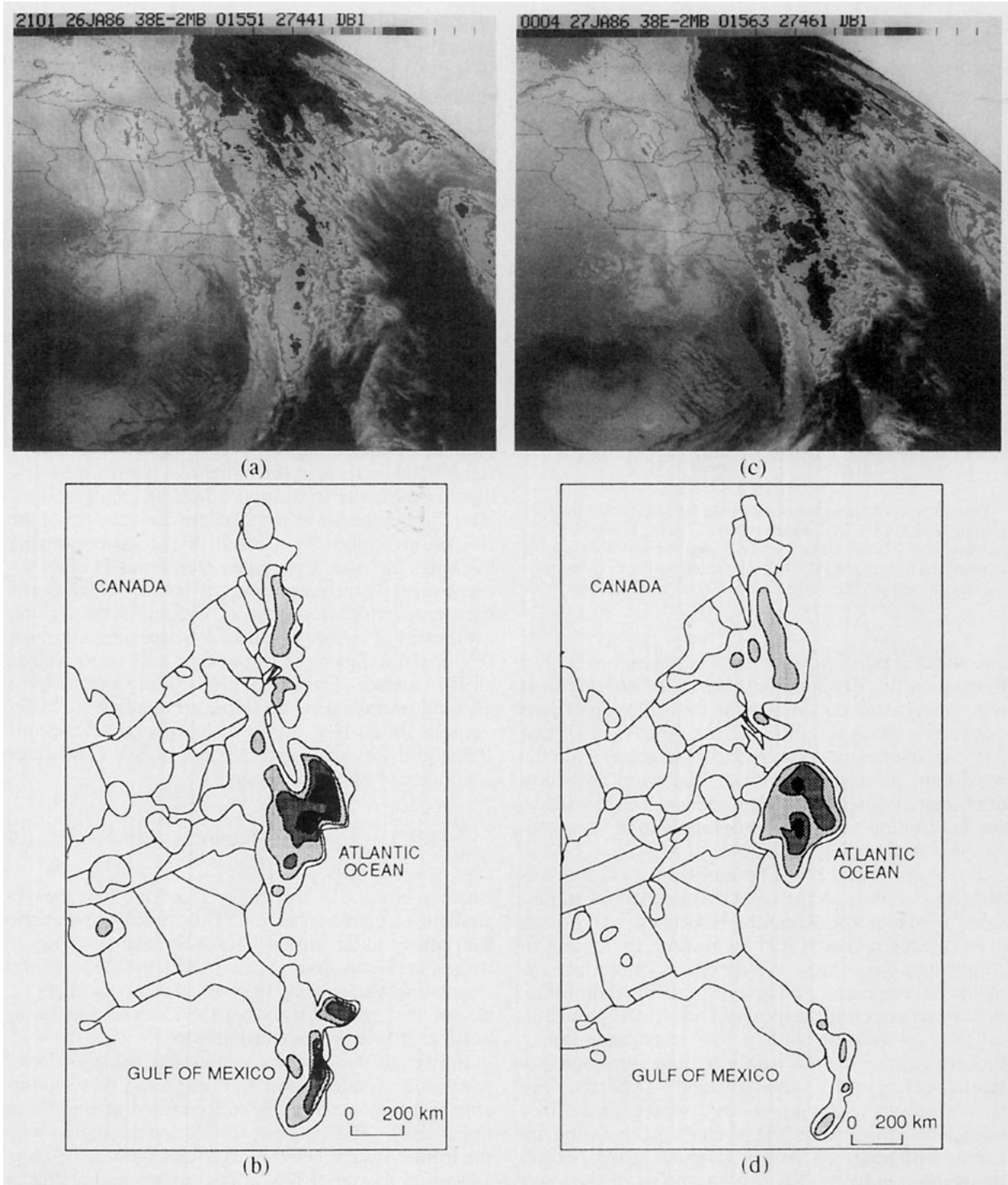

FIG. 14. (a) As for Fig. 1d except for 2100 UTC 26 January 1986. (b) As for Fig. 1c except for 2100 UTC 26 January 1986. (c) As for Fig. 1d except for 0000 UTC 27 January 1986. (d) As for Fig. 1c except for 0000 UTC 27 January 1986.

high-IPV air was counteracted by the diabatic destruction of IPV. Diabatically modulated, differential IPV advection was the result, and this process acted to increase the slope of the dynamic tropopause. To illustrate this we derived the isobaric distribution on the IPV = 3 PVU (1 PVU = 10^{-6} m^2 s^{-1} K kg^{-1}) surface

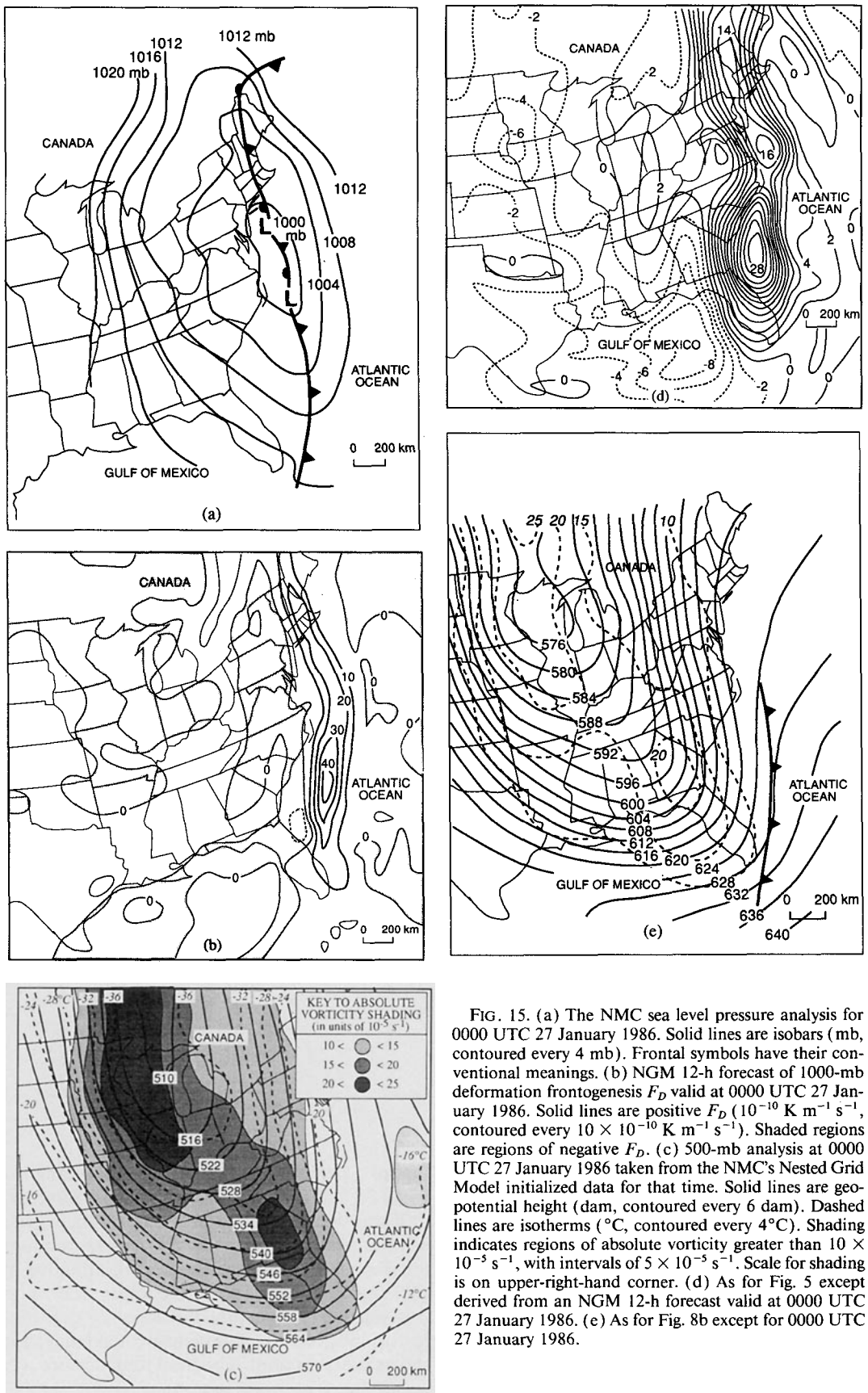

FIG. 15. (a) The NMC sea level pressure analysis for 0000 UTC 27 January 1986. Solid lines are isobars (mb, contoured every 4 mb). Frontal symbols have their conventional meanings. (b) NGM 12-h forecast of 1000-mb deformation frontogenesis F_D valid at 0000 UTC 27 January 1986. Solid lines are positive F_D (10^{-10} K m^{-1} s^{-1}, contoured every 10×10^{-10} K m^{-1} s^{-1}). Shaded regions are regions of negative F_D. (c) 500-mb analysis at 0000 UTC 27 January 1986 taken from the NMC's Nested Grid Model initialized data for that time. Solid lines are geopotential height (dam, contoured every 6 dam). Dashed lines are isotherms (°C, contoured every 4°C). Shading indicates regions of absolute vorticity greater than 10×10^{-5} s^{-1}, with intervals of 5×10^{-5} s^{-1}. Scale for shading is on upper-right-hand corner. (d) As for Fig. 5 except derived from an NGM 12-h forecast valid at 0000 UTC 27 January 1986. (e) As for Fig. 8b except for 0000 UTC 27 January 1986.

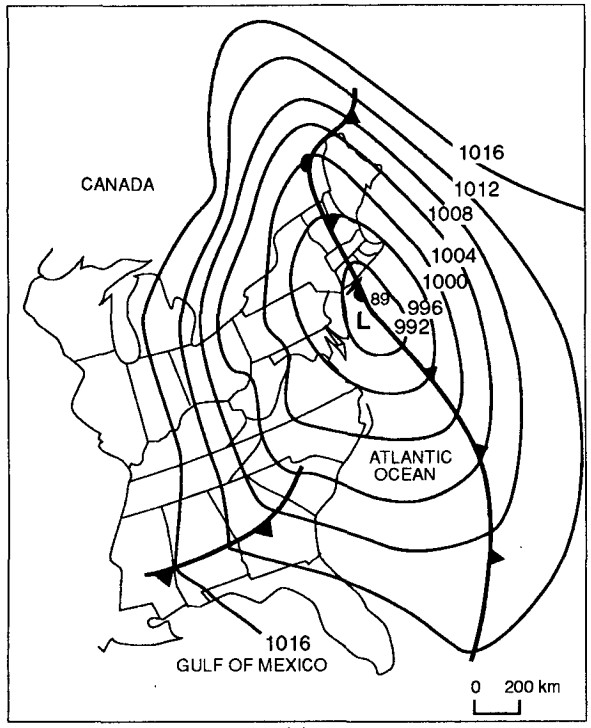

(a)

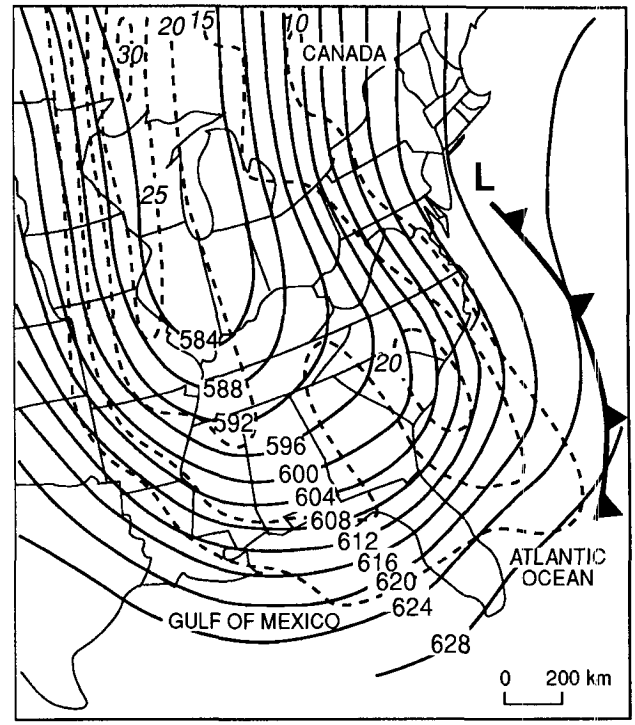

(b)

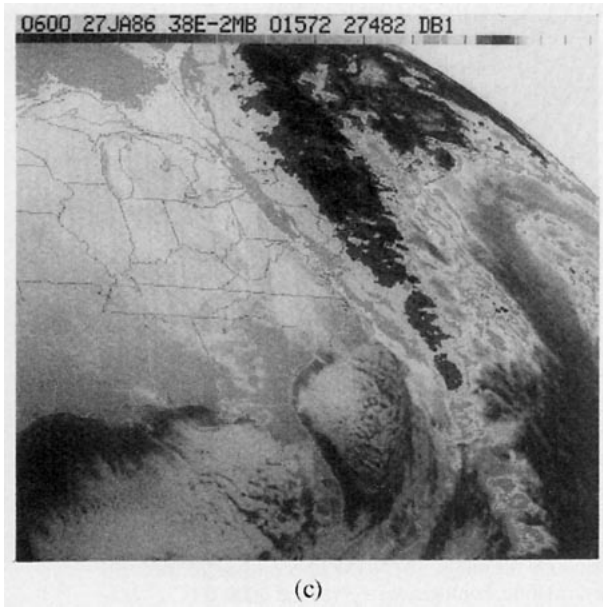

(c)

FIG. 16. (a) As for Fig. 15a except for 0600 UTC 27 January 1986. (b) As for Fig. 8b except for 0600 UTC 27 January 1986. (c) As for Fig. 1d except for 0600 UTC 27 January 1986.

from the NGM data. Although there is no general agreement as to the best IPV surface to associate with the dynamic tropopause, commonly chosen values range from 1 to 2 PVU. We were forced to use 3 PVU, since it was the first IPV surface above 1 PVU that did not exhibit an obvious fold in the vicinity of the surface low. Figure 17 shows the dramatic increase in the slope of the dynamic tropopause, defined in this way, that was coincident with the rapid deepening of the cyclone. Figure 17b, representing the 3-PVU surface at 0600 UTC 27 January, is derived from 6-h forecast data.

If the steepening is to be justly indicted in the development of the low pressure center, the increase in the slope of the tropopause must be attended by stronger warm-air advection in the lower stratosphere, and this warm-air advection must be the dominant term in the local virtual temperature tendency. Figure 18 shows cross sections of virtual temperature advection,

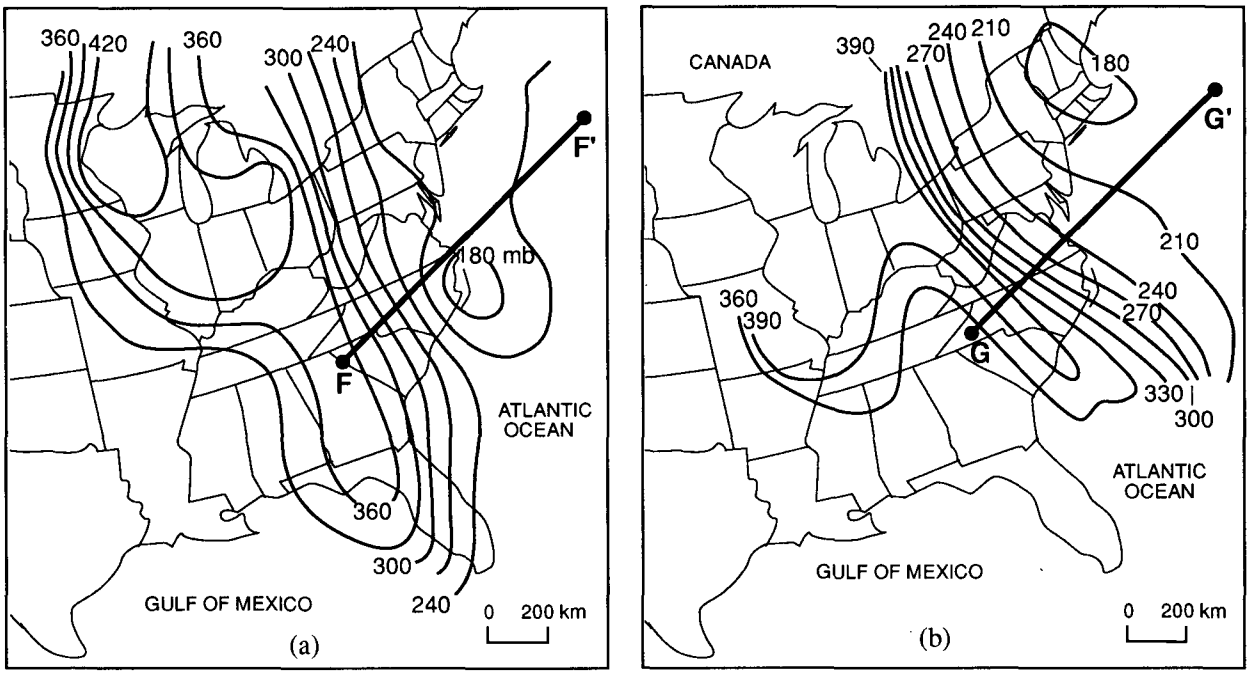

FIG. 17. (a) Topography of the 3-PVU surface at 0000 UTC 27 January 1986 taken from the NGM initialized data. Solid lines are isobars (contoured every 30 mb). Line *FF'* indicates the plane of the cross sections shown in Figs. 18c and 18d. (b) As for (a) except for 0600 UTC 27 January 1986, constructed from 6-h forecast data valid at that time. Line *GG'* indicates the plane of the cross sections shown in Figs. 18e and 18f.

IPV, and total $\partial T_v/\partial t$ at 1800 UTC 26 January and 0000 and 0600 UTC 27 January. Total $\partial T_v/\partial t$ was calculated according to the formula used by Hirschberg and Fritsch (1991):

$$\frac{\partial T_v}{\partial t} = -\mathbf{V}\cdot\nabla T_v + \omega S_a, \tag{4}$$

where the adjusted static stability S_a is given by:

$$S_a = \begin{cases} S_d = -\dfrac{T_v}{\theta_v}\dfrac{\partial \theta_v}{\partial p}, & \text{for } \omega > 0 \text{ or } \mathrm{RH} < 85\% \\ S_m = -\dfrac{T_v}{\theta_e}\dfrac{\partial \theta_e}{\partial p}, & \text{for } \omega < 0 \text{ and } \mathrm{RH} > 85\%. \end{cases}$$

Vigorous convection began only after 1800 UTC. The warm advection maximum of 3.8 K h^{-1} at 200 mb at 1800 UTC (Fig. 18a) was located approximately 400 km upstream of the surface low position. The effect of the vertical velocity at 1800 UTC was to reduce the maximum warming to 2.77 K h^{-1} and relocate it at 300 mb (Fig. 18b), which suggests a dampened effect on the surface development. By 0000 UTC (Fig. 18c) the maximum had increased to 4.8 K h^{-1} and encroached to a position 200 km upstream of the surface low. The vertical velocity served to decrease that effect (lowering the maximum warming to 2.47 K h^{-1} directly over the surface low). Notice the increased tropospheric cooling as a result of the vertical motions (Fig. 18d). Finally, at 0600 UTC (Fig. 18e), when the horizontal map of the tropopause indicated the greatest tropopause slope, the maximum warm advection was 6.4 K h^{-1}, located 200 km upstream of the surface low pressure center. Substantial warming persisted even in the face of the vertical velocity effects (Fig. 18f), as the maximum warming had a magnitude of 4.56 K h^{-1} and was located at 250 mb. As is evident from Fig. 18, directly beneath the regions of largest lower-stratospheric warm-air advection, the upward vertical motion in the troposphere acted to cool the column. The integrated effect of this adiabatic cooling, which occurred at either the moist- or dry-adiabatic lapse rate depending on humidity, was not enough to overcome the warming due to advection in the lower stratosphere. Thus, although vertical motions acted to compensate for the effect of horizontal advection on $\partial T_v/\partial t$, warm-air advection in the lower stratosphere still exerted the largest influence on the local temperature tendency at that level. Also evident from Figs. 18a and 18c is the significant generation of IPV at low levels near the low pressure center, presumably due to the convection. Since deep convection was occurring in the entire region over and east of the surface low by 0600 UTC, the stability was such that each IPV anomaly likely influenced the other, thereby further aiding the rapid

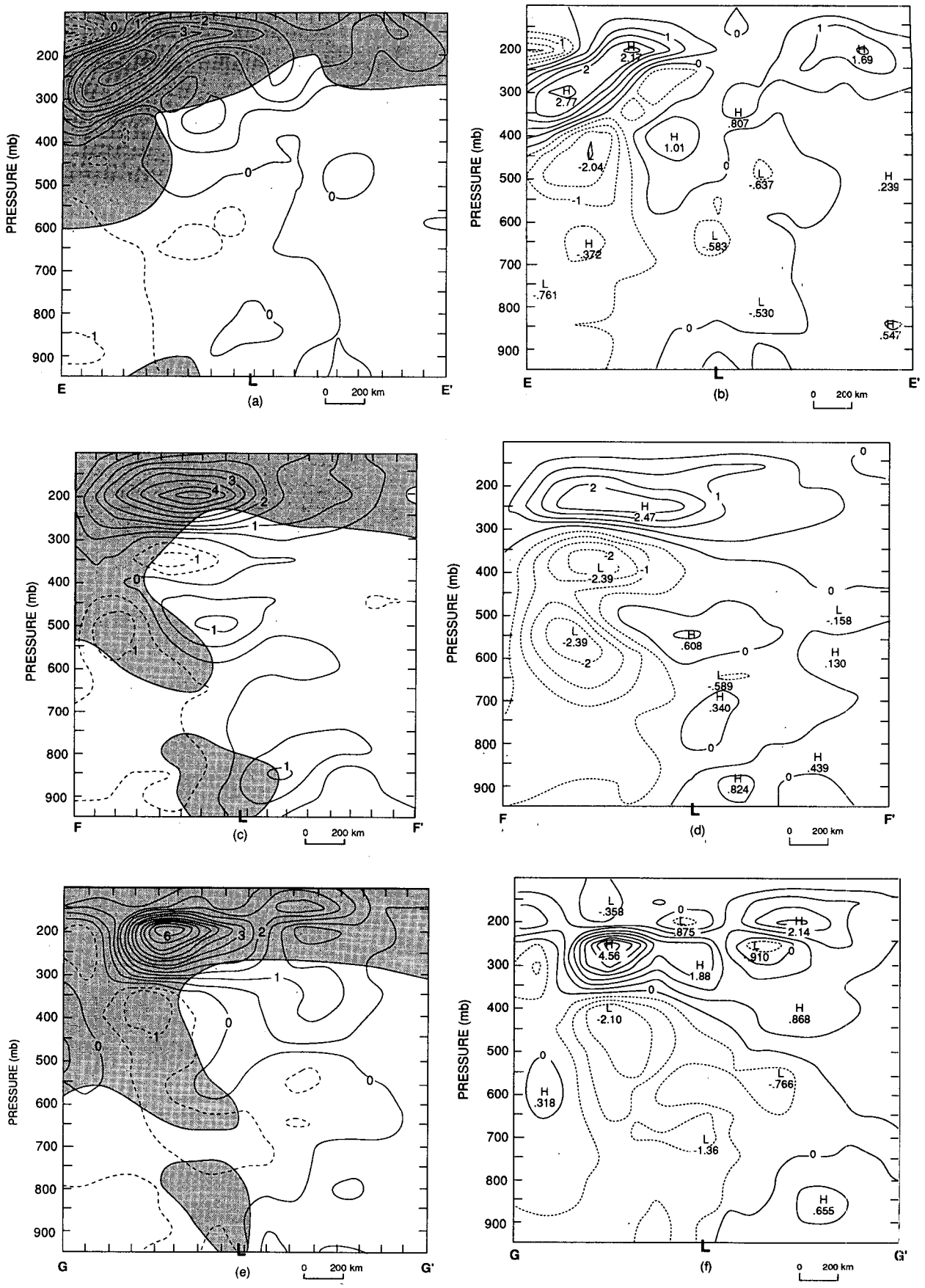
PRESSURE (mb)
200
300
400
500
600
700
800
900
E
E'
L
0 200 km
(a)
H 2.77
H 2.12
H 1.69
H .807
H 1.01
-2.04
L -.637
H .239
H -.372
L .583
L -.761
L -.530
H .547
(b)
F
F'
(c)
H 2.47
L -2.39
L -.158
H .608
H .130
L -.589
H .340
H .439
H .824
(d)
G
G'
(e)
L -.358
H 4.56
H 1.88
H 2.14
L -.910
L -2.10
H .868
L -.766
H .318
L -1.36
H .655
(f)

development of the cyclone in a manner suggested by Hoskins et al. (1985).

4. Discussion of synoptic development

Upper-level fronts are extraordinarily important dynamical entities in the atmosphere. They serve as vorticity-generating systems, as well as one of the main pathways by which the stratosphere and troposphere can interact. They are also important weather-producing phenomena. They have been implicated in cyclogenesis (e.g., Uccellini et al. 1985) and in the production of precipitation bands (Martin et al. 1992).

In this case, the complex interactions between a mobile upper-level front, which formed in the northwesterly flow of a long-wave trough, and a rather weak surface front acted to produce vigorous frontal precipitation that played a significant role in cyclonic development at the surface. The upper-level front was characterized by a frontogenetic horizontal deformation flow that served to maintain the frontal temperature gradient and shear in the face of the forced secondary circulation about the front. When this frontogenetic upper-level flow became parallel to, and to the west of, the surface front, the ageostrophic divergence above the surface front suddenly increased, resulting in a deep column of upward moving air and a rapid increase in the vigor of the frontal precipitation.

The frontal precipitation was further enhanced by the presence of the Gulf Stream, which fed the frontal circulation a steady stream of warm, moist, and potentially unstable air that was quickly converted into deep convection. The tremendous latent heating that resulted at midlevels served to steepen the dynamic tropopause through diabatic destruction of upper-level IPV. As the tropopause steepened, the advection of warm air in the lower stratosphere, just upstream of the surface low pressure center, increased dramatically in intensity. In response to the resulting thickness increases, mass-diverging ageostrophic circulations were induced. These helped to produce the observed 10-mb deepening of the cyclone off the Virginia coast between 0000 and 0600 UTC 27 January. This proposed mechanism strongly resembles a diabatic extension of the "self-development" concept (Sutcliffe and Forsdyke 1950) suggested by Kocin and Uccellini (1990). This concept provides a basis for describing the interaction between dynamic and diabatic processes during rapid cyclogenesis. By warming the troposphere near the axis of the upper-level ridge, the wavelength of the trough–ridge couplet is decreased. This decrease in wavelength tends to increase the divergence aloft by increasing the magnitude of the positive vorticity advection (PVA) aloft. This acts to further intensify the surface low pressure center, which increases the low-level warm air advection and midlevel convective heating. This, in turn, acts to further decrease the wavelength of the trough–ridge couplet in a positive feedback loop between the dynamic and diabatic processes.

The decrease in wavelength of the trough–ridge couplet is evident in the increased slope of the dynamic tropopause. In the present case, this was accomplished by a combination of cold-air advection into the upper trough (i.e., advection of high-IPV air) and diabatic destruction of upper-level IPV due to latent heat release at midtropospheric levels, associated with the burgeoning convective precipitation of the evolving frontal circulation. Thus, the cyclogenesis described here is an example of the self-development mechanism, only here it is recast in terms of IPV and the dynamic tropopause. We believe that the important physical processes described by the self-development theory are made more intuitive when discussed in the context of IPV, the dynamic tropopause, and the effect of tropopause steepness on surface cyclonic development.

The release of latent heat played another important role in this case, namely, to reduce the static stability of the middle troposphere. This decreased stability permitted a constructive interaction between the upper-level IPV anomaly, associated with the upper-level front, and the low-level IPV anomaly, originally associated with the surface front but greatly enhanced by diabatic effects. This interaction likely consisted of mutual amplification of the IPV anomalies, resulting in a more dramatic development of the low pressure center at the surface.

5. Conclusions

The processes that occur in creating the daily weather are extraordinarily complex and are often the result of interactions among many scales of motion. The case described in this paper is an example of such complex interactions. The vertical superposition of two frontal circulations served to initiate vigorous convection. These circulations were themselves embedded within a larger-scale flow associated with a long-wave trough, which served to initiate upper-level frontogenesis and

FIG. 18. (a) Cross section, along line *EE'* in Fig. 11b, of virtual temperature (T_v) advection and IPV calculated from the 6-h forecast data valid at 1800 UTC 26 January 1986. Solid lines are contours of positive T_v advection (K h^{-1}, contoured every 0.5 K h^{-1}). Dashed lines are contours of negative T_v advection (labeled and contoured as for solid lines). Shading indicates region where IPV > 1 PVU. Letter L denotes position of the surface low pressure center. (b) Vertical cross section along line *EE'* in Fig. 11b of total virtual temperature tendency at 1800 UTC 26 January 1986. Contoured as for (a). (c) As for (a) except for 0000 UTC 27 January 1986 using NGM initialization data at that time and along *FF'* in Fig. 17a. (d) As for (b) except along line *FF'* in Fig. 17a and for 0000 UTC 27 January 1986. (e) As for (a) except for 0600 UTC 27 January 1986 using 6-h forecast data valid at that time along line *GG'* in Fig. 17b. (f) As for (b) except along line *GG'* in Fig. 17b and for 0600 UTC 27 January 1986.

to reduce the static stability of the atmosphere east of the trough axis through weak synoptic-scale ascent. Convection occurred on the cumulus scale but, in this case, it was organized by frontogenesis and the resulting vertical circulation. This convection had a considerable effect on the synoptic scale through diabatic destruction of upper-tropospheric–lower-stratospheric IPV and diabatic creation of lower-tropospheric IPV. The destruction of IPV aloft helped to increase the slope of the dynamic tropopause, which, in turn, forced more warm-air advection downstream of the increased slope. The indirect result (described previously) of this increased warm-air advection at upper levels was pressure falls at the surface. Surface cyclonic development on the synoptic scale ensued, aided by the convectively produced low-level IPV and the generally low static stability of the environment.

Acknowledgments. This study was carried out as part of the Genesis of Atlantic Lows Experiment (GALE). It was supported by a series of grants from the Atmospheric Research Section of the National Science Foundation, the latest of which is ATM-8809061.

REFERENCES

Bjerknes, J., 1919: On the structure of moving cyclones. *Geofys. Publ.*, **1**, 1–8.

——, and H. Solberg, 1921: Meteorological conditions for the formation of rain. *Geofys. Publ.*, **2**, 1–60.

——, and H. Solberg, 1922: Life cycle of cyclones and the polar front theory of atmospheric circulation. *Geofys. Publ.*, **3**, 1–18.

Boyle, J. S., and L. F. Bosart, 1986: Cyclone–anticyclone couplets over North America. Part II: Analysis of a major cyclone event over the eastern United States. *Mon. Wea. Rev.*, **114**, 2432–2465.

Danielsen, E. F., 1968: Stratospheric–tropospheric exchange based on radioactivity, ozone, and potential vorticity. *J. Atmos. Sci.*, **25**, 502–518.

Dines, W. H., 1911: The vertical temperature distribution in the atmosphere over England, with some remarks on the general and local circulation. *Phil. Trans. Roy. Soc. London*, **211**, 253–278.

Eliassen, A., 1962: On the vertical circulation in frontal zones. *Geofys. Publ.*, **24**, 147–160.

Hirschberg, P. A., and J. M. Fritsch, 1991: Tropopause undulations and the development of extratropical cyclones. Part I: Overview and observations from a cyclone event. *Mon. Wea. Rev.*, **119**, 496–517.

Hoskins, B. J., and P. Berrisford, 1988: A potential vorticity perspective of the storm of 15–16 October 1987. *Weather*, **43**, 122–129.

——, M. E. McIntyre, and A. W. Robertson, 1985: On the use and significance of isentropic potential vorticity maps. *Quart. J. Roy. Meteor. Soc.*, **111**, 877–946.

Kocin, P. J., and L. W. Uccellini, 1990: Snowstorms along the northeastern coast of the United States: 1955–1985. *Meteor. Monogr.*, No. 44, Amer. Meteor. Soc., 280 pp.

Martin, J. E., J. D. Locatelli, and P. V. Hobbs, 1990: Organization and structure of clouds and precipitation on the mid-Atlantic coast of the United States. Part III: The evolution of a middle-tropospheric cold front. *Mon. Wea. Rev.*, **118**, 195–217.

——, 1992: Organization and structure of clouds and precipitation on the mid-Atlantic coast of the United States. Part V: The role of an upper-level front in the generation of a rainband. *J. Atmos. Sci.*, **49**, 1293–1306.

Miller, J. E., 1948: On the concept of frontogenesis. *J. Meteor.*, **11**, 169–171.

Reed, R. J., 1955: A study of a characteristic type of upper-level frontogenesis. *J. Meteor.*, **12**, 542–552.

——, and F. Sanders, 1953: An investigation of the development of a mid-tropospheric frontal zone and its associated vorticity field. *J. Meteor.*, **10**, 338–349.

Sawyer, J. S., 1956: The vertical circulation at meteorological fronts and its relation to frontogenesis. *Proc. Roy. Soc. London*, **A234**, 346–362.

Sutcliffe, R. C., 1947: A contribution to the problem of development. *Quart. J. Roy. Meteor. Soc.*, **73**, 370–383.

——, and A. G. Forsdyke, 1950: The theory and use of upper air thickness patterns in forecasting. *Quart. J. Roy. Meteor. Soc.*, **76**, 189–217.

Uccellini, L. W., D. Keyser, K. F. Brill, and C. H. Wash, 1985: Presidents' Day cyclone of 18–19 February 1979: Influence of upstream trough amplification and associated tropopause folding on rapid cyclogenesis. *Mon. Wea. Rev.*, **112**, 962–988.